

See discussions, stats, and author profiles for this publication at: <https://www.researchgate.net/publication/30407624>

# Threshold Photoelectron–Photoion Coincidence Spectroscopy of Perfluorocarbons. 2. Unsaturated and Cyclic Perfluorocarbons $C_2F_4$ , $C_3F_6$ , $2-C_4F_8$ , and $c-C_4F_8$

ARTICLE in THE JOURNAL OF PHYSICAL CHEMISTRY A · MAY 1998

Impact Factor: 2.69 · DOI: 10.1021/jp971902y · Source: OAI

---

CITATIONS

34

---

READS

11

4 AUTHORS, INCLUDING:



Chris Mayhew

Indian Institute of Technology Roorkee

63 PUBLICATIONS 818 CITATIONS

SEE PROFILE



Richard P Tuckett

University of Birmingham

162 PUBLICATIONS 2,056 CITATIONS

SEE PROFILE

## Threshold Photoelectron–Photoion Coincidence Spectroscopy of Perfluorocarbons. 2. Unsaturated and Cyclic Perfluorocarbons C<sub>2</sub>F<sub>4</sub>, C<sub>3</sub>F<sub>6</sub>, 2-C<sub>4</sub>F<sub>8</sub>, and c-C<sub>4</sub>F<sub>8</sub>

Gary K. Jarvis,<sup>†</sup> Kenneth J. Boyle,<sup>‡</sup> Chris A. Mayhew,<sup>†</sup> and Richard P. Tuckett<sup>\*,‡</sup>

*Chemical Physics Laboratory, School of Physics and Astronomy, School of Chemistry, University of Birmingham, Edgbaston, Birmingham, B15 2TT, U.K.*

*Received: June 10, 1997; In Final Form: February 18, 1998*

Threshold photoelectron–photoion coincidence (TPEPICO) spectroscopy of three unsaturated (C<sub>2</sub>F<sub>4</sub>, C<sub>3</sub>F<sub>6</sub>, 2-C<sub>4</sub>F<sub>8</sub>) and one cyclic (c-C<sub>4</sub>F<sub>8</sub>) perfluorocarbons has been performed using vacuum-ultraviolet radiation from a synchrotron source in the energy range 10–27 eV. Electrons and ions are detected by threshold electron analysis and time-of-flight mass spectrometry, respectively, allowing breakdown diagrams that show the formation probability of fragment/parent ions as a function of the internal energy of the parent ion to be obtained. Fixed-energy TPEPICO spectra with improved time resolution were performed on some of the fragment ions observed, from which the mean kinetic energy released in fragmentation was determined. High-resolution (ca. 0.01 eV at 10 eV) threshold photoelectron spectra of the three unsaturated species have been recorded, and assignments have been made of the type of electron removed by photoionization to the observed states of the parent ion. Unlike the saturated perfluorocarbons studied in the previous paper, the ground states of C<sub>2</sub>F<sub>4</sub><sup>+</sup>, C<sub>3</sub>F<sub>6</sub><sup>+</sup>, and 2-C<sub>4</sub>F<sub>8</sub><sup>+</sup> are bound in the Franck–Condon region. The first photoelectron band of C<sub>2</sub>F<sub>4</sub> and C<sub>3</sub>F<sub>6</sub> shows vibrational structure associated with the  $\nu_2$  C=C stretching mode. This suggests that upon ionization the C=C bond weakens. From the fragment ions observed by decay of excited states of these three parent ions, there is some correlation between the ions that are observed and the nature of the orbitals from which an electron has been removed. This observation indicates that decay from these states takes place impulsively, and many of these excited states are probably repulsive in the Franck–Condon region. From the c-C<sub>4</sub>F<sub>8</sub> study we have determined a new onset of ionization for c-C<sub>4</sub>F<sub>8</sub> (11.6 ± 0.2 eV) and a new upper limit for the heat of formation at 298 K of C<sub>3</sub>F<sub>5</sub><sup>+</sup> (84 ± 20 kJ mol<sup>−1</sup>).

### 1. Introduction

In the previous paper<sup>1</sup> (referred to as paper 1), we described a study in which threshold photoelectron–photoion coincidence (TPEPICO) spectroscopy was used to study the decay dynamics of the valence electronic states of a series of three positively charged saturated perfluorocarbon (PFC) cations: C<sub>2</sub>F<sub>6</sub><sup>+</sup>, C<sub>3</sub>F<sub>8</sub><sup>+</sup>, and *n*-C<sub>4</sub>F<sub>10</sub><sup>+</sup>. Very similar behavior was observed for all three species, and electronically excited ionic states formed following photoexcitation were found to decay, at least for states below 18 eV, without internal energy conversion. This type of behavior is often termed impulsive dissociation and can arise if the electronic state of the ion to which the species is photoionized is unbound in the Franck–Condon region. This second paper aims to see how a change in structure affects the behavior of such molecules. Thus, the PFCs C<sub>2</sub>F<sub>4</sub>, C<sub>3</sub>F<sub>6</sub>, 2-C<sub>4</sub>F<sub>8</sub>, and c-C<sub>4</sub>F<sub>8</sub> have been studied by TPEPICO spectroscopy to analyze the effects of unsaturation and cyclization. For all four molecules, photoionization mass spectrometry and/or electron impact studies have been performed previously,<sup>2–6</sup> and for C<sub>2</sub>F<sub>4</sub>, C<sub>3</sub>F<sub>6</sub>, and 2-C<sub>4</sub>F<sub>8</sub>, fixed excitation energy photoelectron spectra (PES) have also been published.<sup>7–14</sup> However, no threshold photoelectron or coincidence studies on any of these molecules have been performed to date. The main aim of this study was

to see whether the parent ions of these species decay impulsively, as do their fully saturated counterparts.

### 2. Experimental Section

The apparatus allows for the accumulation and detection of ions in delayed coincidence with threshold photoelectrons formed following ionization of sample gases using monochromatized vacuum-ultraviolet (VUV) radiation from a synchrotron source. Full details are given in paper 1. The majority of the work was carried out using a 1 m Seya monochromator at the Daresbury Laboratory. However, some higher-resolution threshold photoelectron spectra (TPES) were recorded on the 5 m normal-incidence McPherson monochromator at Daresbury. Breakdown diagrams were generated from the data recorded with scanning-energy TPEPICO experiments, giving a representation of the formation probability of the different product ions as a function of the internal energy of the excited parent ion. Mean translational kinetic energy releases for certain fragment ions were determined from TPEPICO spectra recorded with an improved time-of-flight (TOF) resolution. These spectra were recorded at fixed excitation energies corresponding to peaks observed in the scanning TPEPICO spectra. The sample gases C<sub>2</sub>F<sub>4</sub>, C<sub>3</sub>F<sub>6</sub>, 2-C<sub>4</sub>F<sub>8</sub>, and c-C<sub>4</sub>F<sub>8</sub> were obtained commercially (Fluorochem Ltd., UK), having stated purities of >99%, >99%, 97%, and >99%, respectively. The sample of 2-C<sub>4</sub>F<sub>8</sub> was a mixture of the *cis* and *trans* isomers.

\* Author for correspondence: e-mail r.p.tuckett@bham.ac.uk; fax 44 121 414 4426.

<sup>†</sup> School of Physics and Astronomy.

<sup>‡</sup> School of Chemistry.

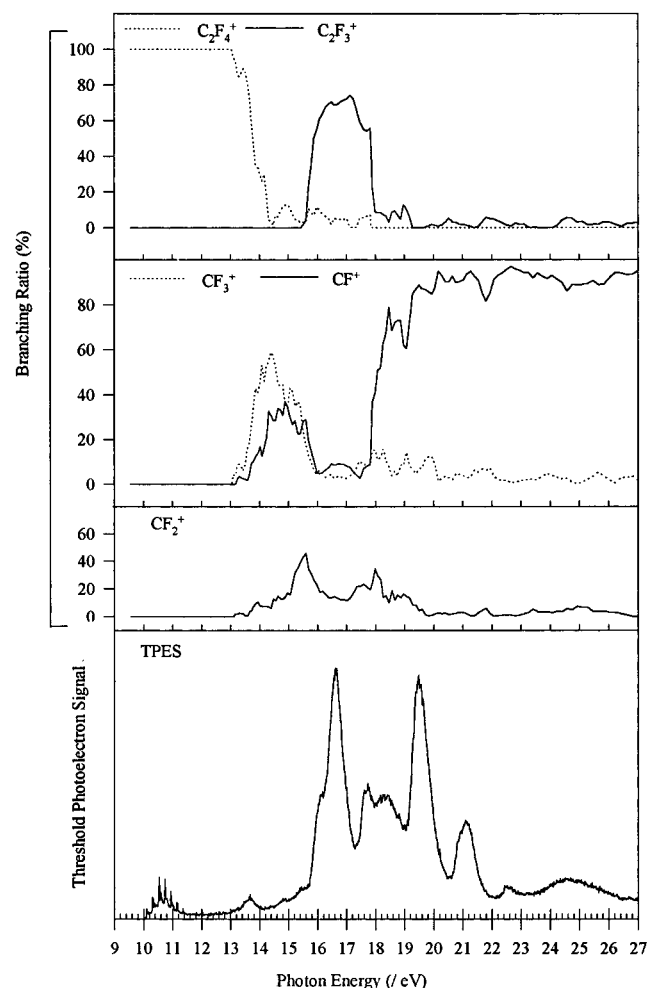


**Figure 1.** Threshold photoelectron spectrum (lower panel) and the corresponding breakdown diagram (upper panels) for  $C_2F_4$ . The optical resolution is 0.15 nm (TPES) and 0.4 nm (breakdown diagram). Mass discrimination effects<sup>1</sup> have been accounted for in the breakdown diagram.

### 3. Results

**3.1.1. TPES of  $C_2F_4$ ,  $C_3F_6$ , and 2- $C_4F_8$ .** The TPES of  $C_2F_4$ ,  $C_3F_6$ , and 2- $C_4F_8$  in the range 10–27 eV with a step size of 17 meV recorded using the 5 m McPherson with an optical resolution of 0.15 nm are shown in Figures 1–3, respectively. In these experiments, second-order radiation from the grating of the monochromator proved to be a problem for two reasons. First, the ground states of all three parent ions are weak under threshold conditions and occur at energies as low as 10 eV where second-order effects are known to exist with this monochromator.<sup>15</sup> Second, at double the ionization energy of the ground state (ca. 20 eV), strong signals are observed from the higher excited states. An attempt was made to account for second-order radiation in the following way. Figure 4a shows both the TPES spectrum of  $C_2F_4$  between 9.4 and 12.0 eV and the spectrum between 18.8 and 24 eV superimposed at half the energy. The intensities are normalized at an energy known to be well below the adiabatic ionization energy (IE). The spectra are then subtracted, yielding the spectrum shown in Figure 4b. The adiabatic IEs of  $C_2F_4$ ,  $C_3F_6$ , and 2- $C_4F_8$  measured after performing this subtraction procedure,  $10.0 \pm 0.2$ ,  $10.6 \pm 0.2$ , and  $11.1 \pm 0.2$  eV, respectively, agree well with previous measurements.<sup>7–14</sup> The ground states of these ions arise from electron removal from the  $\pi$  component of the C=C double bond. The increase in IE with increasing chain length may be

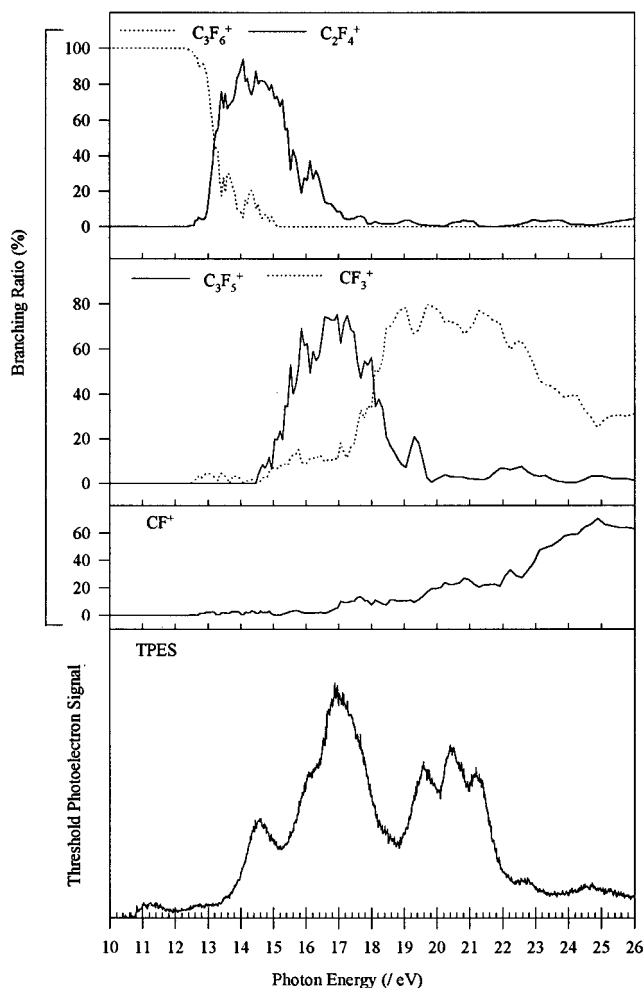


**Figure 2.** Threshold photoelectron spectrum (lower panel) and the corresponding breakdown diagram (upper panels) for  $C_3F_6$ . The optical resolution is 0.15 nm (TPES) and 0.4 nm (breakdown diagram). Mass discrimination effects<sup>1</sup> have been accounted for in the breakdown diagram.

due to the fact that  $CF_3$  groups reduce the  $\pi$  nature of the C=C double bond, thus increasing the perfluoro effect (and hence stability) of the highest occupied molecular orbital (HOMO) of the neutral molecule.<sup>13</sup>

The first photoelectron band of all three molecules is weak compared to the intensity of the higher energy bands, perhaps reflecting a relatively small photoionization cross section to the ground state of the parent ion under threshold electron conditions. In the He I (21.22 eV) PES of these molecules, the first photoelectron band is much more intense relative to the higher energy bands, having roughly the same intensity as the first excited state. The reason for this difference may be that the relative photoionization cross section to the ground state of the parent ion is larger for He I compared to threshold excitation. At higher energies there are further differences between the He I PES and TPES for all three species. In the  $C_2F_4$  TPES, there are three relatively weak peaks between 13.0 and 15.6 eV which are not observed under nonthreshold conditions. These peaks could arise from autoionization of Rydberg states which would be absent in nonresonant PES. In support of this theory, the study by Walter et al.<sup>3</sup> on the photoionization mass spectrum (PIMS) of  $C_2F_4$  does indicate the presence of Rydberg states in this region. Evidence for autoionization effects and/or changes in cross section also occur at 16.4 and 19.5 eV, where an increased intensity of these peaks is observed under threshold

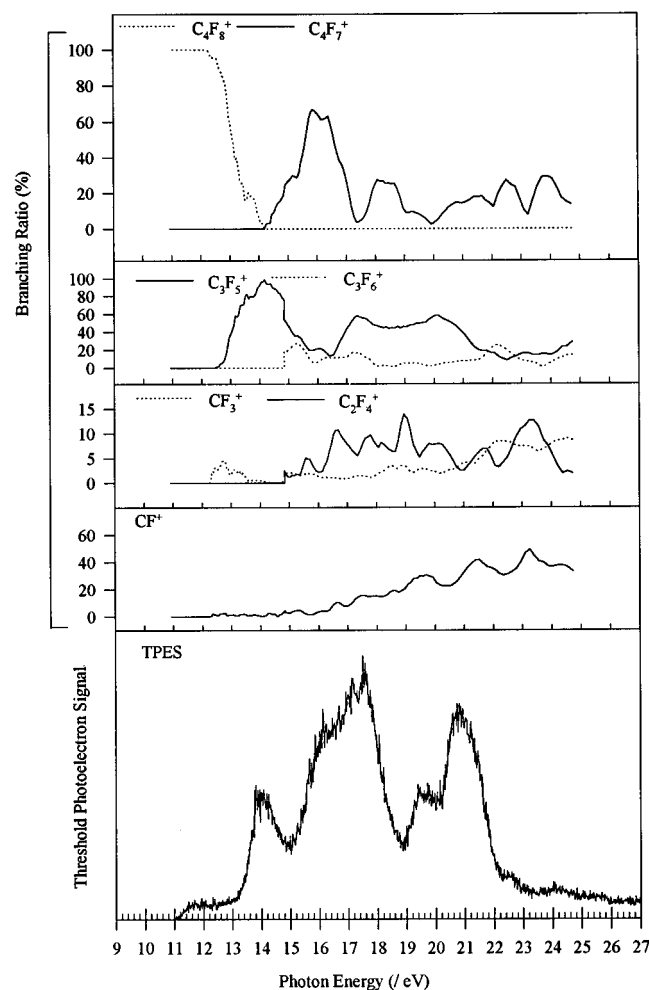


**Figure 3.** Threshold photoelectron spectrum (lower panel) and the corresponding breakdown diagram (upper panels) for 2- $\text{C}_4\text{F}_8$ . The optical resolution is 0.15 nm (TPES) and 0.4 nm (breakdown diagram). Mass discrimination effects<sup>1</sup> have been accounted for in the breakdown diagram.

conditions. For  $\text{C}_3\text{F}_6$  and 2- $\text{C}_4\text{F}_8$ , a similar enhancement for the peak at ca. 19.5 eV is also apparent when its intensity is compared to that in the He I PES.

On comparison of the three TPES, it can be seen that the TPES of  $\text{C}_3\text{F}_6$  and 2- $\text{C}_4\text{F}_8$  are quite similar in shape, with clusters of peaks appearing at similar energies and with similar intensities. The higher-energy bands in  $\text{C}_2\text{F}_4$ , on the other hand, do not show any real similarities with the other two unsaturated PFCs. The reason for this difference is most likely that both  $\text{C}_3\text{F}_6$  and 2- $\text{C}_4\text{F}_8$  have at least one C–C single-bond, whereas  $\text{C}_2\text{F}_4$  has none. As well as being similar to each other, there are also certain similarities above 12 eV between the TPES of  $\text{C}_3\text{F}_6$  and 2- $\text{C}_4\text{F}_8$  and the TPES of the three saturated PFCs studied in paper 1. The first and most obvious likeness is the presence of the three main clusters of peaks, although for the saturated molecules the first band (which corresponds to ionization to the ground state of the parent ion) is comparatively weak. The second photoelectron band for  $\text{C}_3\text{F}_6$  and 2- $\text{C}_4\text{F}_8$  with a threshold at ca. 14 eV corresponds approximately with the onset of ionization of the saturated PFCs. Similarities of this kind allow some approximate assignments of the photoelectron bands, at least to the type of orbital from which an electron is ejected, to be made for the unsaturated species. Such assignments, rough though they may be, prove to be useful probes of the mechanism of decay when used in conjunction with the

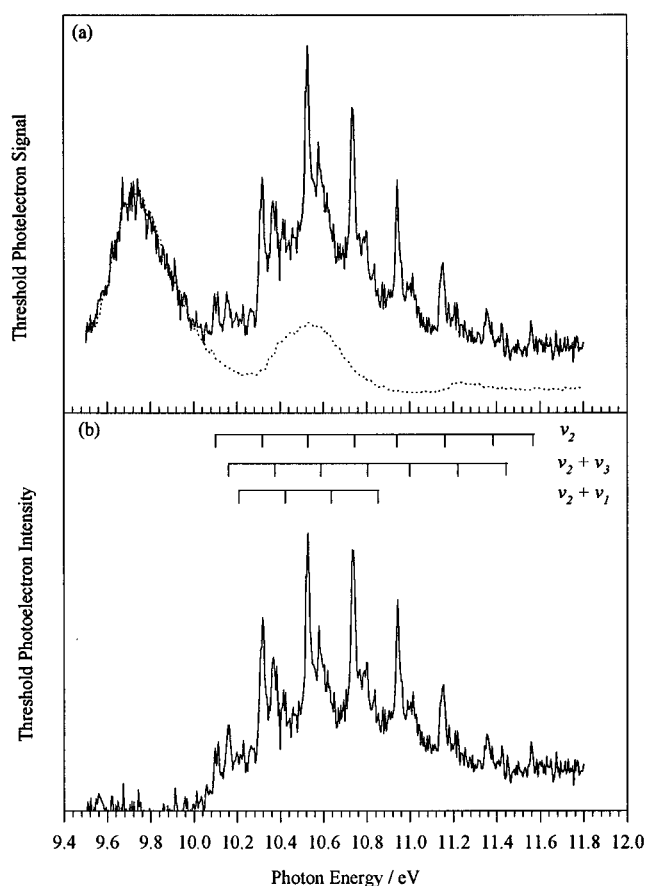


**Figure 4.** High-resolution threshold photoelectron spectrum of the first band of  $\text{C}_2\text{F}_4$ . (a) TPES between 9.4 and 12.0 eV (solid line) and spectrum from 18.8 to 24.0 eV superimposed at half the energy (dotted line). (b) TPES with second-order effects subtracted.

TPEICO spectra (Section 3.3.1.). For example, if a fragment ion is observed in the TPEICO spectrum that corresponds to the product expected from a particular electronic state of the parent ion, then this may indicate that decay is impulsive. Since the ground states of the saturated PFC cations correspond to the removal of an electron from a  $\sigma$ -bonded C–C bond, it therefore seems likely that for  $\text{C}_3\text{F}_6$  and 2- $\text{C}_4\text{F}_8$  the ionic state at this energy also corresponds to electron removal from a similar orbital. The onset of the third photoelectron band of  $\text{C}_3\text{F}_6$  and 2- $\text{C}_4\text{F}_8$ , with a threshold at ca. 15 eV and a peak at ca. 16.4 eV, corresponds well with that of the second photoelectron band of  $\text{C}_2\text{F}_6$ ,  $\text{C}_3\text{F}_8$ , and  $n\text{-C}_4\text{F}_{10}$ . In all cases, electron removal may be from orbitals corresponding to the  $\pi$ -levels of the F atoms delocalized over the C–F bond.<sup>1</sup> A similar assignment can be made for the second photoelectron band of  $\text{C}_2\text{F}_4$  at 16.6 eV which may arise due to electron removal from the delocalized  $\pi$  levels of the F atoms.

Vibrational structure is apparent in the first photoelectron band of  $\text{C}_2\text{F}_4$  (Figure 1). A more detailed spectrum of this band (step size now 5 meV) with the effects of second-order radiation subtracted is shown in Figure 4b. Vibrational structure, albeit much weaker and more poorly defined, is also apparent in the first photoelectron band of  $\text{C}_3\text{F}_6$ , and the analyses of the vibrational progressions in these two bands are shown in Table 1. The vibrational frequencies obtained for  $\text{C}_2\text{F}_4$  are compared with values from other studies. In the  $\text{C}_2\text{F}_4$  spectrum, the main progression has 6–8 members peaking at  $v = 2$ –3 with a separation of 209 meV or  $1686\text{ cm}^{-1}$ . This is assigned to the  $\nu_2$  C=C stretching mode and suggests that the C=C bond length changes upon ionization to this state. By comparison with the

**TABLE 1: Vibrational Wavenumbers Observed in the Ground and Excited States of C<sub>2</sub>F<sub>4</sub><sup>+</sup> and C<sub>3</sub>F<sub>6</sub><sup>+</sup>**

molecule	vertical IE/eV	vibrational wavenumber/cm <sup>-1</sup>			
		vibrational assignt	this work	previous studies	neutral assignt
C <sub>2</sub> F <sub>4</sub>	10.54	$\nu_1$ (C–F stretch)	766	790, <sup>a</sup> 820, <sup>b</sup> 740 <sup>c</sup>	778 <sup>d</sup>
		$\nu_2$ (C=C stretch)	1686	1660, <sup>a</sup> 1710, <sup>b</sup> 1690 <sup>c</sup>	1872 <sup>d</sup>
	17.57	$\nu_3$ (FCF scissors)	371	370, <sup>a</sup> 430 <sup>b</sup>	394 <sup>d</sup>
		$\nu_1$ (C–F stretch)	766	790, <sup>a</sup> 740 <sup>c</sup>	778 <sup>d</sup>
C <sub>3</sub> F <sub>6</sub>	19.41	$\nu_2$ (C=C stretch)		370, <sup>a</sup> 330 <sup>c</sup>	394 <sup>d</sup>
		$\nu_1$ (C–F stretch)	806	790, <sup>a</sup> 740 <sup>c</sup>	778 <sup>d</sup>
	11.0	$\nu_2$ (C=C stretch)	1613	~1600 <sup>e</sup>	1797 <sup>f</sup>

<sup>a</sup> Reference 13. <sup>b</sup> Reference 8. <sup>c</sup> Reference 14. <sup>d</sup> Reference 18. <sup>e</sup> Reference 10. <sup>f</sup> Reference 16.

value of  $\nu_2$  in the neutral (1872 cm<sup>-1</sup>), it is clear that the C=C bond length increases upon ionization as is expected for removal of an electron from a  $\pi$ -bonding orbital. Each  $\nu_2$  peak has a clearly resolved satellite peak at 46 meV or 371 cm<sup>-1</sup> to higher energy which is assigned to the  $\nu_3$  FCF “scissors” mode of vibration. Less clearly resolved, but still apparent for some of the stronger members in the  $\nu_2$  progression, is a satellite at 95 meV or 766 cm<sup>-1</sup> to higher energy. This progression is assigned to the  $\nu_1$  C–F stretching mode. Structure is only observed in one progression in the ground-state photoelectron band of C<sub>3</sub>F<sub>6</sub> with 4–5 members and a vibrational spacing of 200 meV or 1613 cm<sup>-1</sup>. This is assigned to the  $\nu_2$  C=C stretching mode and, as with C<sub>2</sub>F<sub>4</sub>, indicates an increase in C=C bond length upon ionization (the value of  $\nu_2$  in neutral C<sub>3</sub>F<sub>6</sub> is 1797 cm<sup>-1</sup><sup>16</sup>). There are three general comments to make about this vibrational structure. First, the presence of vibrational structure in the ground states of C<sub>2</sub>F<sub>4</sub><sup>+</sup> and C<sub>3</sub>F<sub>6</sub><sup>+</sup> means that the potential energy surfaces of these states are bound in the Franck–Condon region, unlike the corresponding states in the saturated PFC cations. Second, the peak observed at lowest energy in the ground-state TPES band of C<sub>2</sub>F<sub>4</sub> and C<sub>3</sub>F<sub>6</sub> may be due to a higher vibrational level than  $\nu_2 = 0$ . Third, and related to the second point, the maximum in the Franck–Condon envelope is not observed at  $\nu_2 = 0$ , unlike the case in the first photoelectron band of hydrocarbon molecules for which a similar electron is removed.<sup>13,17</sup> This indicates that there is a larger increase in the C=C bond length upon ionization to the ground state of C<sub>2</sub>F<sub>4</sub><sup>+</sup> compared to that of C<sub>2</sub>H<sub>4</sub><sup>+</sup>. Vibrational structure is also partially resolved in the band at 19.4 eV in C<sub>2</sub>F<sub>4</sub> with five members and a spacing of 100 meV or 806 cm<sup>-1</sup>. Activity in this vibrational mode,  $\nu_1$ , suggests that this band in the photoelectron spectrum may arise from electron removal from a C–F bonding orbital. We also observe activity in  $\nu_1$  in the band at 17.6 eV, in agreement with other He I studies.<sup>13,14</sup>

**3.1.2. TPES of c-C<sub>4</sub>F<sub>8</sub>.** The TPES of c-C<sub>4</sub>F<sub>8</sub> in the range 11.6–24.0 eV using the 1 m Seya monochromator with an optical resolution of 0.3 nm is shown in Figure 5. No double bond is present in c-C<sub>4</sub>F<sub>8</sub>, and it is therefore no surprise to observe that the TPES resembles more strongly that of the saturated rather than the unsaturated PFCs with respect to the relative intensity and energies of the bands. No vibrational structure is observed in any band. The onset of ionization<sup>19</sup> which occurs at 11.6 eV is lower than that previously recorded by Bibby et al.<sup>20</sup> of 12.25 eV, who used electron impact ionization mass spectrometry. The reason for this discrepancy is probably related to the inferior resolution of low-energy electron beams compared to photon beams of the same energy. Furthermore, it probably indicates that there is a large change

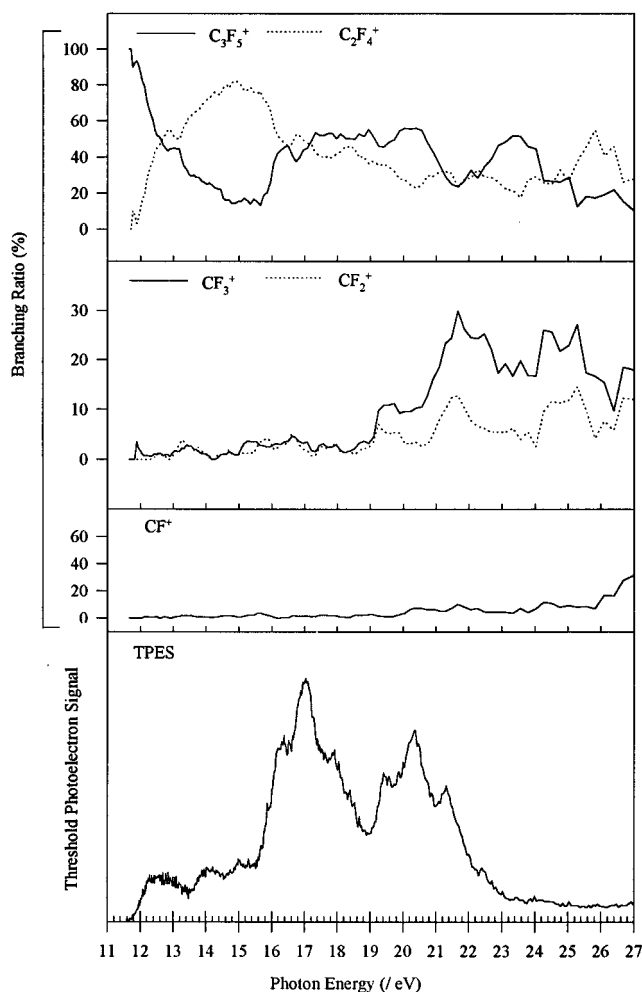


**Figure 5.** Threshold photoelectron spectrum (lower panel) and the corresponding breakdown diagram (upper panels) for c-C<sub>4</sub>F<sub>8</sub>. The optical resolution is 0.3 nm in both cases. Mass discrimination effects<sup>1</sup> have been accounted for in the breakdown diagram.

in geometry in going from c-C<sub>4</sub>F<sub>8</sub> to the ground state of c-C<sub>4</sub>F<sub>8</sub><sup>+</sup> which causes low Franck–Condon factors near threshold.

**3.2. Total Ion Yield Curves.** The total ion signal is recorded during the accumulation of threshold photoelectron spectra, providing a measurement of the total ion production as a function of energy. The ion yields for C<sub>2</sub>F<sub>4</sub>, C<sub>3</sub>F<sub>6</sub>, 2-C<sub>4</sub>F<sub>8</sub>, and c-C<sub>4</sub>F<sub>8</sub> are shown in Figure 6a–d, respectively. As with the TPES, second-order radiation posed a significant problem below ca. 13 eV. Here the problem was more serious since the production of ions is a nonresonant process, so photons of double the energy can produce ions from most of the states seen in the TPES. This can clearly be seen in the figures as a rise of the ion yields to lower energy below ca. 13 eV. As noted in paper 1, the ion yield curve represents the relative ionization cross section across the energy range. If the ionization cross section at any particular energy is similar at threshold to that in excess of threshold where energetic electrons are released and no Rydberg states are present, then by summing the TPES from threshold upward, a curve similar to that observed for the ion yield should be obtained. Discrepancies between the two spectra indicate changes in the photoionization cross section between threshold and nonthreshold conditions and/or the presence of Rydberg states.

For C<sub>2</sub>F<sub>4</sub> (Figure 6a), the agreement between the two curves is reasonable. The first difference to note is the presence of three small peaks in the total ion yield curve at 13.6, 14.8, and

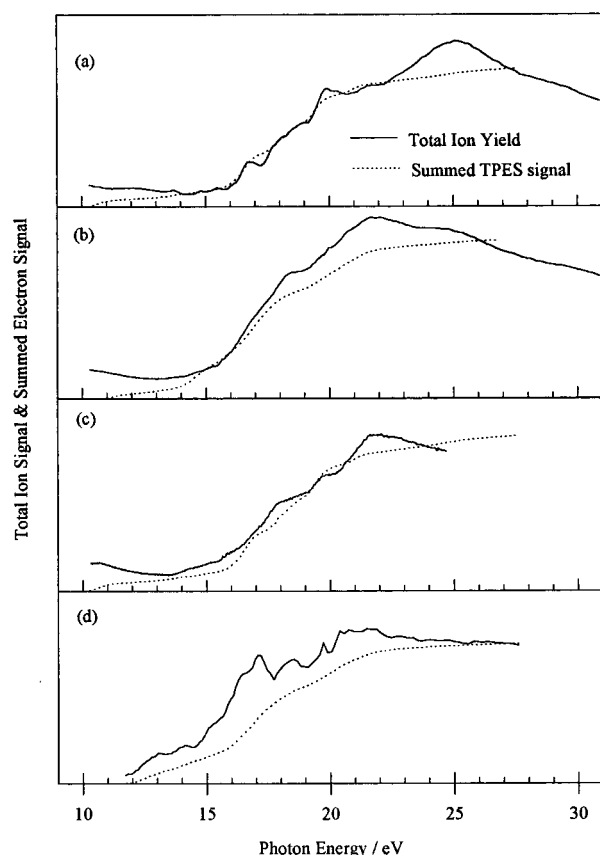


**Figure 6.** Total ion yield and summed TPES signal as a function of energy for (a)  $\text{C}_2\text{F}_4$ , (b)  $\text{C}_3\text{F}_6$ , (c)  $2\text{-C}_4\text{F}_8$ , and (d)  $\text{c-C}_4\text{F}_8$ . The summed TPES signal at energy  $E$  is the integral of the individual TPES channels from threshold to  $E$ .

15.4 eV, indicating that autoionization is occurring. This confirms that the extra peaks observed in the TPES (Figure 1) at these energies arise due to autoionization of Rydberg states emitting near-zero-energy electrons. The sharp decline in the ion yield between ca. 16.8–17.4 and ca. 20–21 eV also indicates the presence of Rydberg states between 16.2–16.8 and 19–20 eV, respectively; once an autoionization feature has passed, the ion yield will recede down to the ion yield expected for direct ionization. In the TPES, an enhancement in the intensity of the two peaks at these latter positions compared with the He I PES has already been noted. At ca. 22 eV, there is a rapid increase in the total ion yield compared to the integrated TPES signal peaking at ca. 25 eV, which is then followed by a steady decline to higher energies. Since both effects are shallow, it is more likely that they are caused by changes in the photoionization cross section than by autoionization. For  $\text{C}_3\text{F}_6$  and  $2\text{-C}_4\text{F}_8$  (Figure 6b,c), a similar change in photoionization cross section occurs over this region with an initial rise in the ion yield at ca. 20 eV followed by a decline at higher energies. We note further that the agreement between the  $\text{C}_3\text{F}_6$  and  $2\text{-C}_4\text{F}_8$  ion yields compared to their corresponding summed TPES signal is generally poor over the whole energy region. However, it should be noted that mass discrimination as described in paper 1 may also play a role in the deviations between the two sets of data, and this effect will be more pronounced for the heavier PFCs.

For  $\text{c-C}_4\text{F}_8$  (Figure 6d) many peaks are apparent in the ion yield at 13.0, 14.0, 17.2, and 18.6 eV. These peaks most likely indicate the presence of Rydberg states at these energies.

**3.3. Fragmentation of the Valence States of  $\text{C}_2\text{F}_4^+$ ,  $\text{C}_3\text{F}_6^+$ ,  $2\text{-C}_4\text{F}_8^+$ , and  $\text{c-C}_4\text{F}_8^+$ .** TPEPICO spectra in the energy-

**TABLE 2: Dissociation Channels and Appearance Energies of Ions Formed from  $\text{C}_2\text{F}_4$ ,  $\text{C}_3\text{F}_6$ ,  $2\text{-C}_4\text{F}_8$ , and  $\text{c-C}_4\text{F}_8$**

parent molecule	dissociation channel	dissociation energy/eV	appearance energy/eV <sup>a</sup>
$\text{C}_2\text{F}_4$	$\text{C}_2\text{F}_4^+$	10.10	10.1(0.2)
	$\text{C}_2\text{F}_3^+ + \text{F}$	<15.85	15.6(0.1)
	$\text{CF}_3^+ + \text{CF}$	13.44	13.2(1.0)
	$\text{CF}_2^+ + \text{CF}_2$	14.00	13.2(1.0)
	$\text{CF}^+ + \text{CF}_3$	13.81	13.5(1.0)
	$\text{CF}^+ + \text{CF}_2 + \text{F}$	17.28	13.5(1.0)
$\text{C}_3\text{F}_6$	$\text{C}_3\text{F}_6^+$	10.60	10.6(0.2)
	$\text{C}_3\text{F}_5^+ + \text{F}$	<13.79 <sup>b</sup>	14.6(0.3)
	$\text{C}_2\text{F}_4^+ + \text{CF}_2$	12.81	12.4(0.5)
	$\text{CF}_3^+ + \text{C}_2\text{F}_3$	13.64	14.6(2.0)
	$\text{CF}^+ + \text{C}_3\text{F}_5$	14.16	14.6(2.0)
	$\text{CF}^+ + \text{C}_2\text{F}_4 + \text{F}$	17.40	14.6(2.0)
$2\text{-C}_4\text{F}_8$	$2\text{-C}_4\text{F}_8^+$	11.05	11.1(0.2)
	$\text{C}_4\text{F}_7^+ + \text{F}$	? <sup>c</sup>	14.2(0.4)
	$\text{C}_3\text{F}_6^+ + \text{CF}_2$	13.39	14.8(0.5)
	$\text{C}_3\text{F}_5^+ + \text{CF}_3$	<13.11 <sup>b</sup>	12.4(0.6)
	$\text{C}_2\text{F}_4^+ + \text{C}_2\text{F}_4$	13.02	14.8(2.0)
	$\text{CF}_3^+ + \text{C}_3\text{F}_5$	12.64	12.2(2.0)
$\text{c-C}_4\text{F}_8$	$\text{CF}^+ + \text{C}_3\text{F}_7$	15.04	
	$\text{C}_3\text{F}_5^+ + \text{CF}_3$	<12.24 <sup>b</sup>	11.6(0.2)
	$\text{C}_2\text{F}_4^+ + \text{C}_2\text{F}_4$	12.15	11.8(0.5)
	$\text{CF}_3^+ + \text{C}_3\text{F}_5$	11.77	
	$\text{CF}_2^+ + \text{C}_3\text{F}_6$	13.34	
	$\text{CF}^+ + \text{C}_3\text{F}_7$	14.17	

<sup>a</sup> Appearance energies were determined from their first onset. Errors are given in parentheses. <sup>b</sup> Values determined from the upper limit of the heat of formation of  $\text{C}_3\text{F}_5^+$  from Anicich et al.<sup>22</sup> of 126 kJ mol<sup>-1</sup>. From the first onset of  $\text{C}_3\text{F}_5^+$  from  $\text{c-C}_4\text{F}_8$ , we have redetermined this value to be  $84 \pm 20$  kJ mol<sup>-1</sup> (see section 3.2.2 of text). <sup>c</sup> Heat of formation of  $\text{C}_4\text{F}_7^+$  not known.

scanning mode were recorded from 9.6 to 27.5 eV with a step size of 0.4 nm for  $\text{C}_2\text{F}_4$  and  $\text{C}_3\text{F}_6$ , from 10.9 to 24.8 eV with a step size of 0.4 nm for  $2\text{-C}_4\text{F}_8$ , and from 9 to 25.4 eV for  $\text{c-C}_4\text{F}_8$  with a step size of 0.5 nm. The optical resolution of the Seya monochromator was 0.4 nm, except for the  $\text{c-C}_4\text{F}_8$  measurement for which it was 0.3 nm. The ions observed and the corresponding breakdown diagrams are shown in Figures 1–3 for the unsaturated species and Figure 5 for  $\text{c-C}_4\text{F}_8$ . Second-order radiation was again a concern for energies below ca. 13 eV. In most cases it was obvious when second order was responsible for the appearance of certain ions at low energies, these ions having appearance energies far below their predicted thermodynamic threshold. In the breakdown diagrams the contribution of ions produced by second-order radiation in the range 10–13 eV has been subtracted. Mass discrimination effects, as described in paper 1, have also been incorporated into these figures.

The experimentally determined appearance energies and corresponding lowest possible dissociation energies for all of the fragment ions produced from the four PFCs are shown in Table 2. Most of the thermochemical data are taken from Lias et al.<sup>21</sup> Exceptions are the heats of formation of  $\text{C}_3\text{F}_5^+$  (<126 kJ mol<sup>-1</sup>) taken from Anicich et al.,<sup>22</sup> that of  $n\text{-C}_3\text{F}_7$  (–1282 kJ mol<sup>-1</sup>) from Bryant,<sup>23</sup> that of  $\text{C}_3\text{F}_5$  (–762 kJ mol<sup>-1</sup>) from Sauers et al.,<sup>24</sup> that of  $\text{c-C}_4\text{F}_8$  (–1515 kJ mol<sup>-1</sup>) from Benson et al.,<sup>25</sup> and that of  $\text{CF}_3^+$  (383 kJ mol<sup>-1</sup>) from Jarvis et al.<sup>1</sup> The heats of formation are for 298 K and use the stationary electron convention to define the heat of formation of a cation.<sup>26</sup> The determination of onsets for certain ions appearing at energies corresponding to Franck–Condon gaps in the TPES is difficult and leads to sizable errors. This may account for the inconsistencies and large errors seen in the appearance energies of  $\text{CF}_3^+$ ,  $\text{CF}_2^+$ , and  $\text{CF}^+$  from  $\text{C}_2\text{F}_4$ , since between 11 and 15 eV Franck–Condon factors are small. The same phenomenon can

perhaps explain the small discrepancies seen in Table 2 for the production of  $C_2F_4^+$  from  $C_3F_6$  and of  $CF_3^+$  from 2- $C_4F_8$ . This effect illustrates that the error in the determination of appearance thresholds by TPEPICO spectroscopy can be large, and this is an inferior technique to PIMS<sup>27</sup> in determining such quantities. Note that for the  $C_2F_4$  study to have an appearance energy as low as 13.5 eV (Table 2)  $CF^+$  must be formed in combination with  $CF_3$ , which can only form via fluorine migration across the C=C bond.

**3.3.1.  $C_2F_4^+$ ,  $C_3F_6^+$ , and 2- $C_4F_8^+$ .** The fragmentation patterns of  $C_2F_4^+$ ,  $C_3F_6^+$ , and 2- $C_4F_8^+$  prove to be very interesting. The first point to note is that, unlike the saturated PFCs, the ground state of these ions results in the production of the parent ion. This state must therefore be bound within the Franck–Condon region. The second point is that fragmentation of some of these higher energy states of all three ions leads to products that reflect the type of orbital from which an electron has been removed. This is characteristic of impulsive decay. As examples, we consider the second photoelectron band at 16.5 eV for  $C_2F_4$  from which  $C_2F_3^+$  is the major product (Figure 1). This correlates with the fact that this state may arise from electron removal from the  $\pi$  levels of the F atoms that are delocalized over the C–F bond (from comparison with the saturated PFCs<sup>1</sup>). Note also that, as expected for impulsive behavior, the onset of the two features occurs within experimental error, at the same energy. The second photoelectron band of 2- $C_4F_8$  at 14 eV leads almost exclusively to the production of  $C_3F_5^+$  (Figure 3). Again, this is in agreement with the assignments of the photoelectron spectrum (section 3.1.1). The second photoelectron band of  $C_3F_6$  at 14.6 eV dissociates predominantly to  $C_2F_4^+$  (Figure 2). In light of the previous discussion, it seems likely that this ion is formed by a mechanism involving the lengthening of the  $\sigma$  (C–C) bond and  $F^-$  migration prior to dissociation, rather than by direct cleavage of the C=C double bond. The reason  $C_2F_3^+$  is not formed at this energy is thermodynamic; the  $C_2F_4^+ + CF_2$  channel at 12.81 eV is energetically open, whereas the  $C_2F_3^+ + CF_3$  channel at 15.09 eV is closed. Note also that an  $F^-$  jump is not necessary with 2- $C_4F_8$ , since the  $C_3F_5^+ + CF_3$  channel at 12.68 eV is open.

We now consider the third photoelectron band. For  $C_3F_6$  and 2- $C_4F_8$ , this state between 15 and 18 eV corresponds to electron removal from a C–F bond (section 3.1.1). Therefore, impulsive dissociation would predict  $C_3F_5^+$  and  $C_4F_7^+$  to be the predominant ion products, and this is what is observed. Interestingly, the energy at which the threshold takes place, ca. 15 eV, corresponds almost exactly with the C–F bond-breaking feature in all the saturated PFCs<sup>1</sup> and in  $C_2F_4$ . The third band of  $C_2F_4$  between 17 and 19 eV dissociates to form  $CF^+$ , and no comment can be made about the decay mechanism.

The fourth photoelectron band for  $C_3F_6$  and 2- $C_4F_8$  between 19 and 22 eV leads predominantly to production of  $CF_3^+$  and of  $C_3F_5^+$  and  $CF_3^+$ , respectively. If dissociation is impulsive, this suggests that electron removal to form these excited states of  $C_3F_6^+$  and 2- $C_4F_8^+$  may again occur from an orbital that is essentially  $\sigma$  (C–C) bonding. The fourth photoelectron band of  $C_2F_4^+$  between 19 and 20 eV leads to production of  $CF^+$ , and again no comment can be made as to the mechanism of decay.

To summarize, the implication of these findings for the unsaturated PFC cations is that the majority of states above the ground state are likely to be unbound, with decay occurring rapidly before energy randomization can take place. This is

obviously not the case for all the excited states of  $C_2F_4^+$ , since vibrational structure is present in the bands at 17.6 and 19.4 eV.<sup>13,14</sup>

**3.3.2. c- $C_4F_8^+$ .** Figure 5 shows that the parent ion is not present at any energy, indicating that as with the saturated PFCs<sup>1</sup> the ground state of c- $C_4F_8^+$  is unbound in the Franck–Condon region. The fragment ion produced at threshold is  $C_3F_5^+$ . The data in Table 2 therefore imply that the upper limit on the heat of formation of this ion given by Anicich and Bowers<sup>22</sup> is too high. We have used the procedure of Traeger et al.<sup>26</sup> to relate the first onset of  $C_3F_5^+$  from c- $C_4F_8$  at 298 K to the heat of formation of this cation at this temperature. Allowing for the calculated internal energy of  $C_3F_5^+$  and  $CF_3$ , we obtain a new upper limit of  $\Delta H_f^\circ(298\text{ K})$  for  $C_3F_5^+$  of  $84 \pm 20\text{ kJ mol}^{-1}$ . Note that the production of this ion necessitates two C–C bonds to break and a fluorine to migrate, and it is surprising that  $CF_3^+ + C_3F_5$  does not also form. As the photon energy increases from threshold, the yield of  $C_3F_5^+$  decreases and that of  $C_2F_4^+$  increases. There is a sharp increase in the  $C_3F_5^+$  signal at 15.7 eV, corresponding to the threshold of a strong peak in the TPES, perhaps suggesting impulsive behavior in this state of c- $C_4F_8^+$ . Surprisingly,  $C_4F_7^+$  does not form at this photon energy as expected from comparison with all the other PFC species, and this may arise due to the instability of the cyclic  $C_4F_7^+$  ion that is formed. From 2- $C_4F_8$ ,  $C_4F_7^+$  can be stabilized by delocalization of the electron that was initially involved with the double bond; this is obviously not possible for c- $C_4F_8$ .

**3.4. Kinetic Energy Released in Fragmentation for  $C_2F_4^+$ ,  $C_3F_6^+$ , 2- $C_4F_8^+$ , and c- $C_4F_8^+$ .** TPEPICO TOF spectra in the nonscanning mode were measured at the energies shown in Table 3 corresponding to some of the maxima seen in the TPES in Figures 1–3 and 5. In all cases, a TOF resolution of 16 ns per channel was used. Table 3 also shows the experimentally determined mean total kinetic energies,  $\langle E_T \rangle$ , the fraction of available energy deposited into translation of the fragments, and the calculated fractional releases for both pure impulsive and statistical decay. These calculations are described in paper 1. Fixed-energy TPEPICO TOF spectra were also recorded for the formation of parent ions at 10.49, 11.81, and 12.49 eV for  $C_2F_4$ ,  $C_3F_6$ , and 2- $C_4F_8$ , respectively. The broadening of the parent ion peak can only be due to thermal effects. The peak shape is predicted to be Gaussian, with a full width at half-maximum (fwhm) which is only a function of the mass of the ion, the temperature, and the extraction field.<sup>29</sup> Our values for the fwhm of the parent ions are consistent with a temperature of  $350 \pm 50\text{ K}$ , in agreement with that expected for a slow effusion of gas into the interaction region of our apparatus through a hyperdermic needle.<sup>30</sup>

For fragmentation of  $C_2F_4$  into  $C_2F_3^+ + F$  at 16.48 eV, the high KE released (Table 3) strongly suggests that the process is impulsive. However, the fractional KE release ( $0.89 \pm 0.17$ ) is too high to be accounted for by the pure impulsive model. There are three possible explanations. First, the heat of formation of  $C_2F_3^+$  used in the thermochemical data of Table 2 ( $791\text{ kJ mol}^{-1}$ ) is an upper limit,<sup>21</sup> and it may be that the  $C_2F_3^+ + F$  dissociation limit occurs at a lower energy than 15.85 eV. If this is the case,  $E_{\text{avail}}$  is greater than 0.63 eV, thereby reducing the fractional KE release. Second,  $C_2F_4^+$  is decaying by a “modified impulsive” mechanism. In this model, the bonds of the departing fragments are considered as being rigid, and energy is only deposited into rotation and translation.<sup>31</sup> Third, the decay is statistical but proceeds via a barrier in the exit channel. For a simple C–F bond-breaking channel, however, we believe that this mechanism is unlikely. For the production of  $CF_2^+$  from

**TABLE 3: Comparison of Mean Total Kinetic Energy Releases from Experimental Results and Calculated from Statistical and Impulsive Dissociation Models<sup>a</sup>**

parent ion	daughter ion	hν/eV	<i>E</i> <sub>avail</sub> /eV	total <i>E</i> <sub>T</sub> /eV <sup>b</sup>	fraction		
					expt <sup>b</sup>	statistical	impulsive
C <sub>2</sub> F <sub>4</sub> <sup>+</sup>	C <sub>2</sub> F <sub>3</sub> <sup>+</sup>	16.48	>0.63	0.56(0.11)	<0.89(0.17)	0.08	0.48
	CF <sub>2</sub> <sup>+</sup>	16.59	2.59	0.33(0.07)	0.13(0.02)	0.08	0.24
	CF <sub>2</sub> <sup>+</sup>	17.72	3.72	0.47(0.12)	0.13(0.03)	0.08	0.24
	CF <sup>+</sup>	19.48	5.66	0.36(0.05)	0.06(0.01)	0.08	0.28
	CF <sup>+</sup>	21.05	7.23	0.52(0.07)	0.07(0.01)	0.08	0.28
	CF <sup>+</sup>	22.58	8.76	0.68(0.11)	0.08(0.01)	0.08	0.28
C <sub>3</sub> F <sub>6</sub> <sup>+</sup>	C <sub>2</sub> F <sub>4</sub> <sup>+</sup>	15.02	2.21	0.33(0.06)	0.15(0.03)	0.05	0.18
	C <sub>3</sub> F <sub>5</sub> <sup>+</sup>	17.36	4.01 <sup>c</sup>	1.26(0.37)	0.31(0.10)	0.05	0.44
	CF <sub>3</sub> <sup>+</sup>	20.4	6.99	0.41(0.04)	0.06(0.01)	0.05	0.16
2-C <sub>4</sub> F <sub>8</sub> <sup>+</sup>	C <sub>3</sub> F <sub>5</sub> <sup>+</sup>	14.02	1.34 <sup>c</sup>	0.40(0.07)	0.30(0.07)	0.03	0.13
	C <sub>3</sub> F <sub>5</sub> <sup>+</sup>	17.6	4.92 <sup>c</sup>	0.42(0.09)	0.09(0.03)	0.03	0.13
	C <sub>3</sub> F <sub>5</sub> <sup>+</sup>	20.63	7.95 <sup>c</sup>	0.48(0.07)	0.06(0.01)	0.03	0.13
	CF <sub>3</sub> <sup>+</sup>	21.12	8.72	0.37(0.05)	0.04(0.01)	0.03	0.13
c-C <sub>4</sub> F <sub>8</sub> <sup>+</sup>	C <sub>2</sub> F <sub>4</sub> <sup>+</sup>	12.7	0.56	0.08(0.01)	0.14(0.01)	0.03	0.12
	C <sub>2</sub> F <sub>4</sub> <sup>+</sup>	14.86	2.72	0.26(0.07)	0.10(0.02)	0.03	0.12
	C <sub>2</sub> F <sub>4</sub> <sup>+</sup>	16.82	4.68	0.36(0.03)	0.08(0.01)	0.03	0.12
	C <sub>3</sub> F <sub>5</sub> <sup>+</sup>	20.18	8.37 <sup>c</sup>	0.58(0.17)	0.07(0.02)	0.03	0.13

<sup>a</sup> Method of analysis<sup>28</sup> assumes a two-body fragmentation. <sup>b</sup> Errors are given in parentheses. <sup>c</sup> Determined using our new upper limit (84 kJ mol<sup>-1</sup>) for the heat of formation of C<sub>3</sub>F<sub>5</sub><sup>+</sup>.

C<sub>2</sub>F<sub>4</sub>, the fractional KE release is higher than the statistical limit but lower than the prediction of the pure impulsive model. Whether this indicates that the molecule is behaving statistically, since the statistical release in the table only gives a lower limit, or that CF<sub>2</sub><sup>+</sup> and/or CF<sub>2</sub> are formed with an extra amount of vibration caused by an increase in C–F bond length upon ionization of C<sub>2</sub>F<sub>4</sub> cannot be determined from the data. Interpretation of the KE releases into CF<sup>+</sup> from C<sub>2</sub>F<sub>4</sub> at energies above 19.5 eV is difficult, because the method of analysis<sup>28</sup> assumes a two-body fragmentation. CF<sub>3</sub> can only be formed in partnership with CF<sup>+</sup> following F<sup>-</sup> migration across the C=C bond, and it is not clear whether such a complex fragmentation mechanism is appropriate to be treated by the method of Powis et al.<sup>28</sup> which assumes a simple bond cleavage.

The KE releases for C<sub>3</sub>F<sub>6</sub><sup>+</sup> suggest that fragmentation to C<sub>2</sub>F<sub>4</sub><sup>+</sup> and C<sub>3</sub>F<sub>5</sub><sup>+</sup> is most probably of an impulsive nature (agreeing with the conclusion from section 3.3) and energy is partitioned as for the pure impulsive model. For CF<sub>3</sub><sup>+</sup> production, however, only a low fractional KE release is observed, indicating either that decay from this state is statistical or that the fragments formed from an impulsive mechanism are left with internal vibration.

For 2-C<sub>4</sub>F<sub>8</sub> and c-C<sub>4</sub>F<sub>8</sub>, the difference between the fractional KE release predicted by the pure impulsive model and the statistical model is small on account of the size of the molecules, making exact determination of the type of behavior impossible. For most cases of the fragment ions, the observed fractional release appears to fall between the releases predicted by the two extremes.

#### 4. Conclusions

This study has provided some evidence for nonstatistical decay taking place for all the perfluorocarbon cations studied in this series from some of their excited electronic states. For the unsaturated PFC cations, the ground state is bound, and the parent ion is therefore observed in the TPEPICO spectrum at the appropriate energy. The consequence of impulsive behavior from many of the excited electronic states of these cations may mean that these states are unbound in the Franck–Condon region. These findings may have implications on the understanding of the “perfluoro effect” noted by Brundle et al.,<sup>13</sup> by which σ molecular orbitals are stabilized by 2–4 eV by the

substitution of H by F whereas the stabilization of π molecular orbitals is generally of a smaller magnitude. Brundle et al. conclude that σ orbitals are delocalized over the F atoms and are strongly stabilized by the high effective nuclear charge of the F atoms. Although this effect may be taking place to some extent for the PFC molecules studied here, it would seem that the greater effect of fluorination is to shift the equilibrium geometry of the parent ion relative to the ground state of the neutral to longer bond lengths. In other words, removal of an electron from a fluorinated system has a more dramatic effect on bond lengths than removal of an electron from a hydrocarbon. This will result in a shift of the bound part of the potential surface of the cation out of the Franck–Condon region, as is observed in many cases.

This effect is greatest for the saturated PFCs and is demonstrated by the fact that no parent ion has ever been observed. For the unsaturated species the effect is less but can still be seen as a long vibrational progression in ν<sub>2</sub> in the ground state of C<sub>2</sub>F<sub>4</sub><sup>+</sup>. The Franck–Condon maximum does not occur at ν<sub>2</sub> = 0 as it does for production of C<sub>2</sub>H<sub>4</sub><sup>+</sup> from C<sub>2</sub>H<sub>4</sub>,<sup>17</sup> therefore indicating a change in geometry in the fluorinated species is occurring upon ionization. The increase in ionization energy and apparent reduction in the photoionization cross section for the series C<sub>2</sub>F<sub>4</sub>, C<sub>3</sub>F<sub>6</sub>, and 2-C<sub>4</sub>F<sub>8</sub> can also be explained by the idea that the CF<sub>3</sub> groups reduce the π nature of the C=C double bond, thus increasing the perfluoro effect of the HOMO of the neutral molecule.

**Acknowledgment.** We thank NERC, EPSRC, and the Daresbury Laboratory for a Research Grant, Research Studentships (G.K.J., K.J.B.), and a CASE award (K.J.B.). We also thank Dr. I. Powis (Nottingham University) for the use of his kinetic energy analysis program and Dr. P. A. Hatherly (Reading University) for technical advice on the apparatus. Finally, we thank Professor J. M. Dyke (Southampton University) for sending us a copy of his unpublished He I PES of C<sub>3</sub>F<sub>6</sub>.

#### References and Notes

- (1) Jarvis, G. K.; Boyle, K. J.; Mayhew, C. A.; Tuckett, R. P. *J. Phys. Chem. A* **1998**, *102*, 3219.
- (2) Berman, D. W.; Bomse, D. S.; Beauchamp, J. L. *Int. J. Mass Spectrom. Ion Phys.* **1981**, *39*, 263.



- (3) Walter, T. A.; Lifshitz, C.; Chupka, W. A.; Berkowitz, J. J. *Chem. Phys.* **1969**, 51, 3531.
- (4) Dewar, M. J. S.; Worley, S. D. *J. Chem. Phys.* **1969**, 50, 654.
- (5) Lifshitz, C.; Long, F. A. *J. Phys. Chem.* **1965**, 69, 3731.
- (6) Lifshitz, C.; Long, F. A. *J. Phys. Chem.* **1963**, 67, 2463.
- (7) Dyke, J. M. Private communication.
- (8) Sell, J. A.; Kupperman, A. *J. Chem. Phys.* **1979**, 71, 4703.
- (9) Sell, J. A.; Mintz, D. M.; Kupperman, A. *Chem. Phys. Lett.* **1978**, 58, 601.
- (10) Freiser, B. S.; Beauchamp, J. L. *J. Am. Chem. Soc.* **1974**, 96, 6260.
- (11) Wittel, K.; Bock, H. *Chem. Ber.* **1974**, 107, 317.
- (12) Robin, M. B.; Taylor, G. N.; Kuebler, N. A.; Bach, R. D. *J. Org. Chem.* **1973**, 38, 1049.
- (13) Brundle, C. R.; Robin, M. B.; Kuebler, N. A.; Basch, H. *J. Am. Chem. Soc.* **1972**, 94, 1451.
- (14) Lake, R. F.; Thompson, H. *Proc. R. Soc. London A* **1970**, A315, 323.
- (15) Holland, D. M. P.; West, J. B.; MacDowell, A. A.; Munro, I. H.; Beckett, A. G. *Nucl. Instrum. Methods Phys. Res. B* **1989**, 44, 233.
- (16) Nielson, J. R.; Claassen, H. H.; Smith, D. C. *J. Chem. Phys.* **1952**, 20, 1916.
- (17) Baker, A. D.; Baker, C.; Brundle, C. R.; Turner, D. W. *Int. J. Mass Spectrom. Ion Phys.* **1968**, 1, 285.
- (18) Nielson, J. R.; Claassen, H. H.; Smith, D. C. *J. Chem. Phys.* **1950**, 18, 812.
- (19) See ref 22 of paper 1.
- (20) Bibby, M. M.; Carter, G. *Trans. Faraday Soc.* **1963**, 59, 2455.
- (21) Lias, S. G.; Bartmess, J. E.; Liebman, J. F.; Holmes, J. L.; Levin, R. D.; Mallard, W. G. *J. Phys. Chem. Ref. Data, Suppl. 1* **1988**, 17.
- (22) Anicich, V. G.; Bowers, M. T. *Int. J. Mass Spectrom. Ion Phys.* **1974**, 13, 359.
- (23) Bryant, W. M. *J. Polym. Sci.* **1962**, 56, 278.
- (24) Sauers, I.; Christophorou, L. G.; Carter, J. G. *J. Chem. Phys.* **1974**, 71, 3016.
- (25) Benson, S. W.; O'Neal, H. E. *Natl. Stand. Ref. Data Ser., Natl. Bur. Stand.* **1970**, 21.
- (26) Traeger, J. C.; McLaughlin, R. G. *J. Am. Chem. Soc.* **1981**, 103, 3647.
- (27) Asher, R. L.; Ruscic, B. *J. Chem. Phys.* **1997**, 106, 210.
- (28) Powis, I.; Mansell, P. I.; Danby, C. J. *Int. J. Mass Spectrom. Ion Phys.* **1979**, 32, 15.
- (29) Franklin, J. L.; Hierl, P. M.; Whan, D. A. *J. Chem. Phys.* **1967**, 47, 3184.
- (30) Hatherly, P. A.; Smith, D. M.; Tuckett, R. P. *Z. Phys. Chem. (Munich)* **1996**, 195, 97.
- (31) Busch, G. E.; Wilson, K. R. *J. Chem. Phys.* **1972**, 56, 3626.